Supporting Information

Three-Dimensional Microphase Separation and Synergistic Permeability in Stacked Lipid-Polymer Hybrid Membranes

Minjee Kang[†], Byeongdu Lee[‡], and Cecilia Leal*[†]

† Department of Materials Science and Engineering, University of Illinois at Urbana-Champaign, Urbana, Illinois 61801, United States
‡ X-ray Science Division, Argonne National Laboratory, Argonne, Illinois 60439, United States

*(C.L.) E-mail: cecilial@illinois.edu

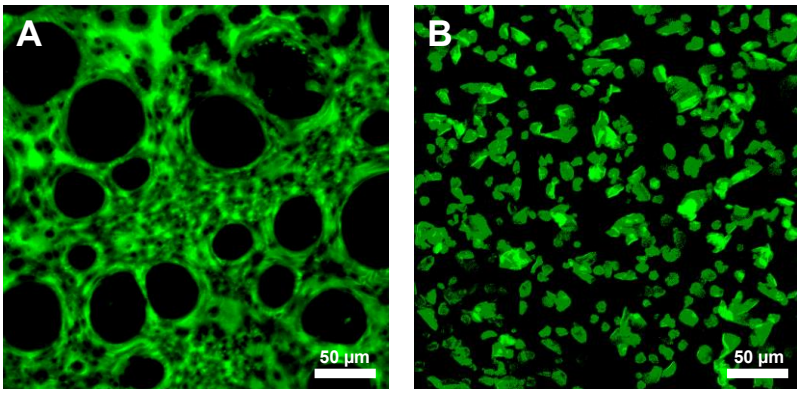

Figure S1. Confocal Laser Scanning Microscope (CLSM) Images of hybrid films in water doped with 0.1 mol% NBD-DPPE (A) 4:1 molar ratio of DPPC to PBD-b-PEO (B) 1:1 molar ratio of DPPC to PBD-b-PEO. The scale bars = 50 µm.

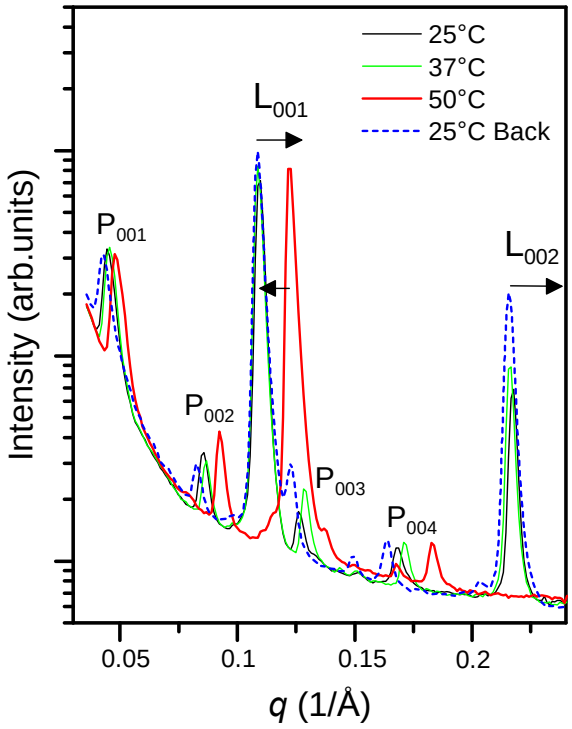

Figure S2. One-dimensional GISAXS $I(q)$ plots for the hybrid 4:1 molar ratio of DPPC to PBD-b-PEO membranes equilibrated at different temperatures. Note the position of (001), (002) peaks associated with DPPC lipids upon temperature changes in comparison to the PBD-b-PEO polymer peaks. The transition

temperature of DPPC lipids at which they undergo a transition from the gel to liquid phase is 41°C. Reflecting such a characteristic temperature, the DPPC peak positions do not change below 41°C but do move above 41°C. Upon cooling, the DPPC peaks go back to the original q positions. In contrast to the response of DPPC lipids to the temperature changes, PBD-b-PEO polymers with a glass transition temperature below 25°C show no changes in the peak locations at all temperatures tested. That is, the two sets of lamellar peaks–each associated with lipids or polymers–show a response to temperature changes that is characteristic to the corresponding phase; this further supports the coexistence of lipid-rich and polymer-rich domains in the hybrid membranes.

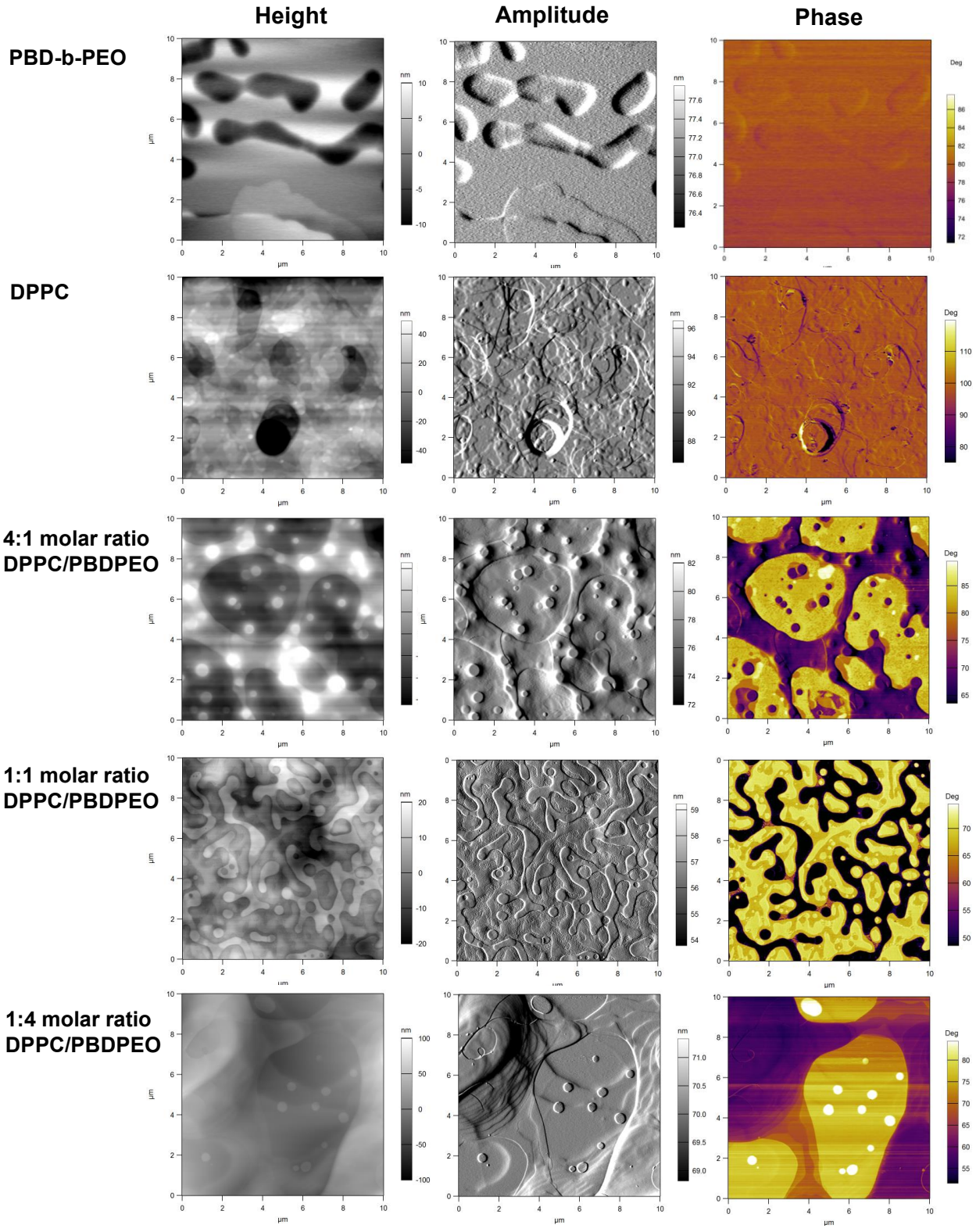
Height
Amplitude
Phase
PBD-b-PEO
DPPC
4:1 molar ratio
DPPC/PBDPEO
1:1 molar ratio
DPPC/PBDPEO
1:4 molar ratio
DPPC/PBDPEO
µm
nm
Deg

Figure S3. AFM tapping mode images of PBD-b-PEO films, DPPC films, 4:1 molar ratio DPPC/PBD-b-PEO films, 1:1 molar ratio DPPC/PBD-b-PEO films, 1:4 molar ratio DPPC/PBD-b-PEO films in height, amplitude, and phase mode. The scanned surface area was 100 μm^2.

5 mol% PTX incorporated

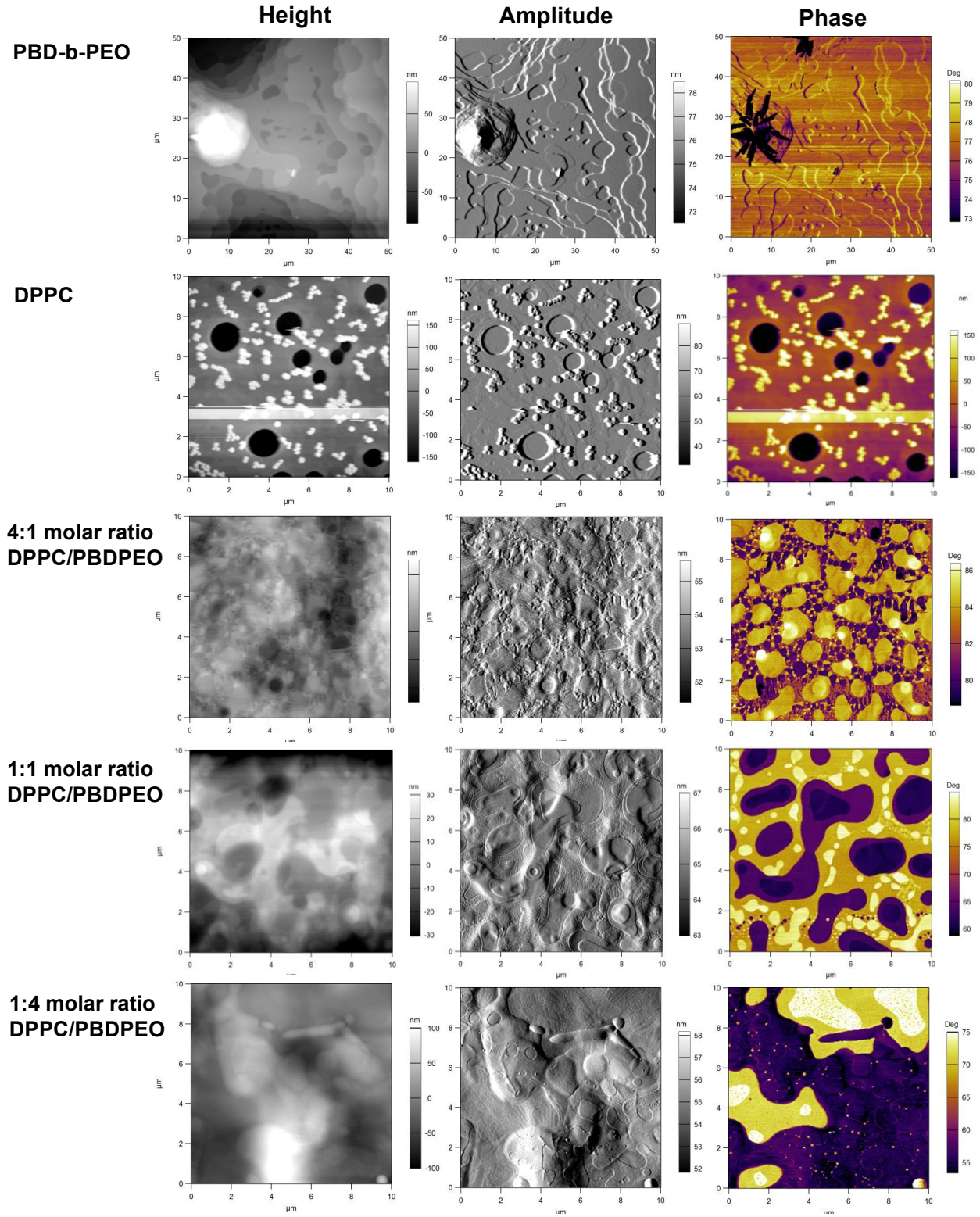

Figure S4. AFM tapping mode images of paclitaxel (PTX)-incorporated (5 mol%) PBD-b-PEO films, DPPC films, 4:1 molar ratio DPPC/PBD-b-PEO films, 1:1 molar ratio DPPC/PBD-b-PEO films, 1:4 molar ratio DPPC/ PBD-b-PEO films in height, amplitude, and phase mode. The scanned surface area was 100 μm^2 except PBD-b-PEO films (2500 μm^2).

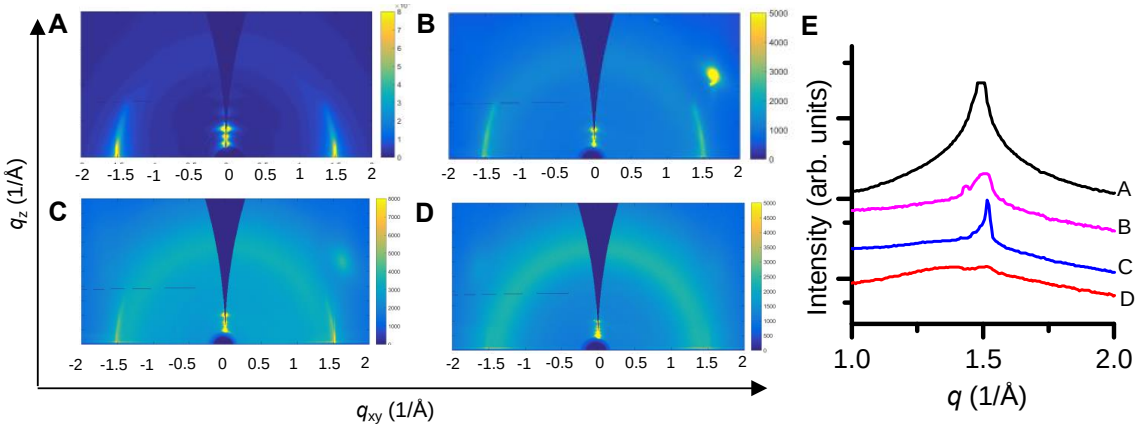

Figure S5. (A-D) GIWAXS two-dimensional reciprocal space images of the PTX-incorporating films: (A) DPPC + 5 mol% PTX (B) 4:1 molar ratio of DPPC to PBD-b-PEO + 5 mol% PTX (C) 1:1 DPPC: PBD-b-PEO + 5 mol% PTX (D) 1:4 DPPC: PBD-b-PEO + 5 mol% PTX (E) GIWAXS one-dimensional I(q) profiles of (A-D) films.

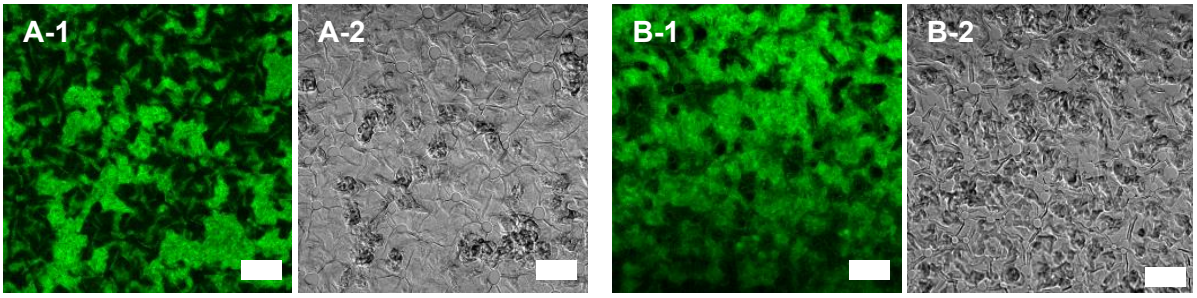

Figure S6. (A, B) CLSM images of 1:1 molar ratio of DPPC to PBD-b-PEO hybrid films with 5 mol% PTX, doped with 0.2 mol% PTX-Oregon Green 488. (A-1, B-1) PTX-Oregon Green 488 Channel. (A-2, B-2) Bright-field images. Scale bars = 20 µm.

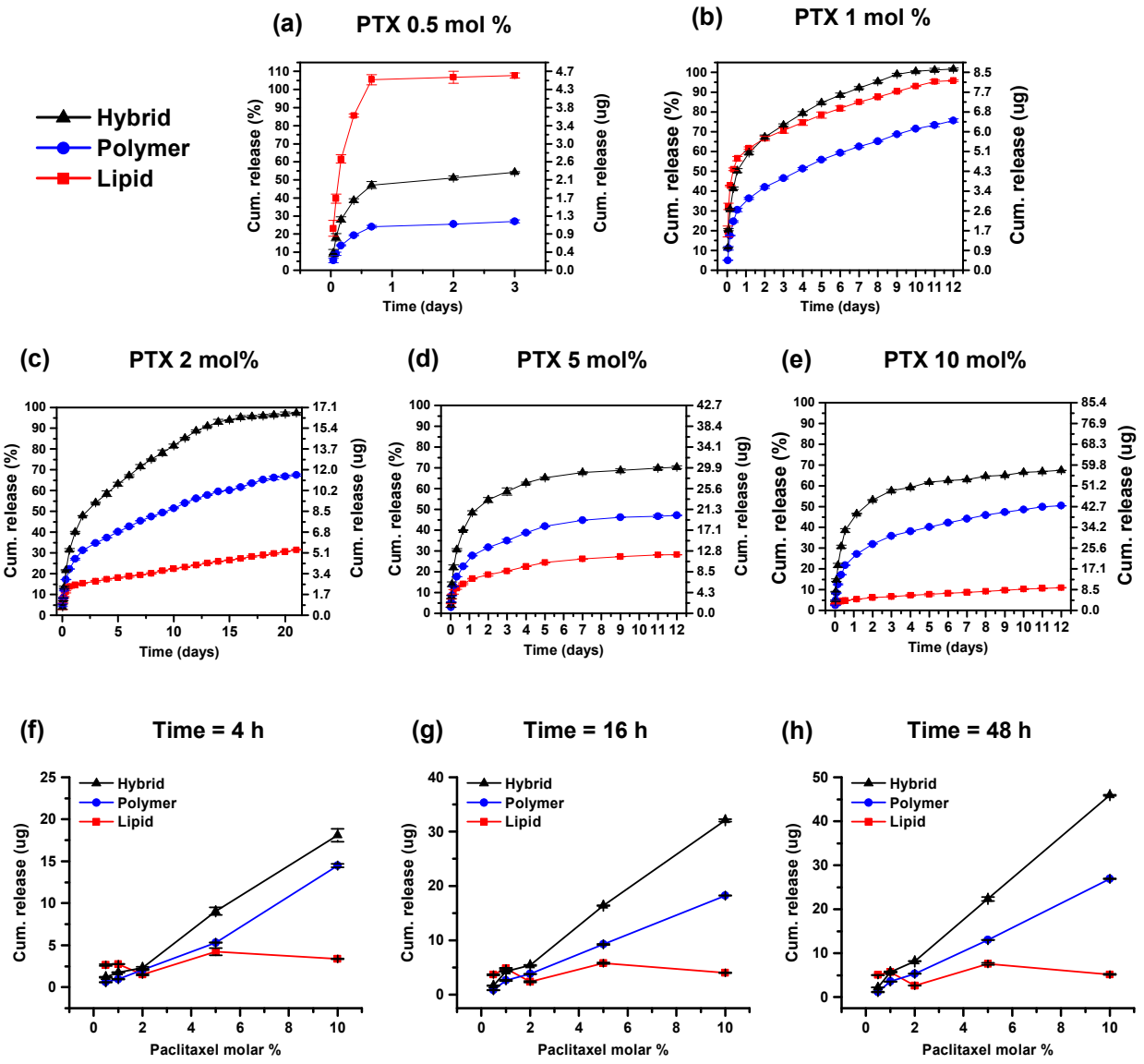

Figure S7. Cumulative release profiles of PTX from 1:1 molar ratio of DPPC to PBD-b-PEO hybrid films. (a-e) The left axis represents the % release, and the right axis shows the released mass (µg). The mass of the hybrid film was kept the same for all conditions and only the molar % of PTX to the film was varied. The lipid films displayed a burst release when a low molar percent of PTX was incorporated. (a, b) During the first 1 hour period, 20 % of PTX is released from the lipid films. (c-e) On the other hand, the lipid films showed slow release when a high molar percent of PTX was added, which could be attributed to the formation of PTX crystals. The hybrid films presented faster PTX release rates compared to lipid and polymer films. (f-h) Cumulative PTX release amount (µg) from each film at certain time points. Note

that the release amount of PTX from the polymer and hybrid films increased showing a linear behavior upon increase in molar % of PTX incorporated, which was not the case for lipid-only films. Each point represents the arithmetic mean ± SD, *n* =3.

Sample	Molar percent of PTX loaded in the films				
	0.5	1	2	5	10
Lipid	95.9	97.3	98.5	95.9	98.5
Polymer	96.1	96.0	98.5	98.8	98.5
Hybrid	98.3	95.8	99.5	98.7	97.5

Table S1. PTX loading efficiencies (%) of different films with varying amount of PTX loaded. The hybrid films comprise 1:1 molar ratio of DPPC to PBD-b-PEO. The loading efficiency was defined by the following equation: loading efficiency (%) = (total amount of drug – free drug in the medium)/total amount of drug × 100.

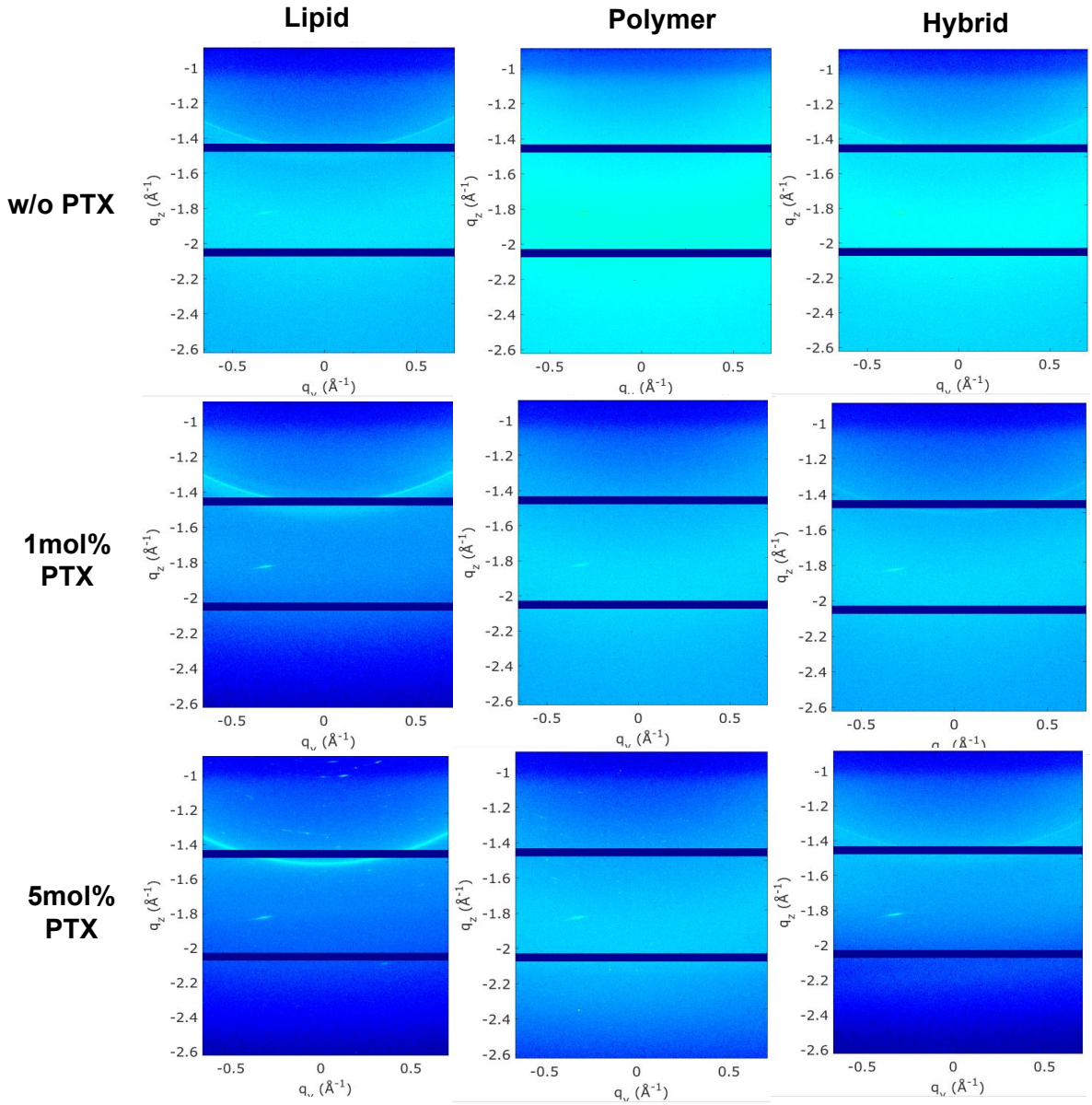

Figure S8. Transmission WAXS two-dimensional data of liposomes, polymersomes, and hybrid vesicles without PTX incorporated and with 1 and 5 mol% PTX incorporated. Besides the lipid tail ordering diffraction at ≈ 1. 5 $Å^{-1}$, the liposomes and polymersomes incorporating 5 mol% PTX showed a number of diffraction spots associated with PTX crystals.

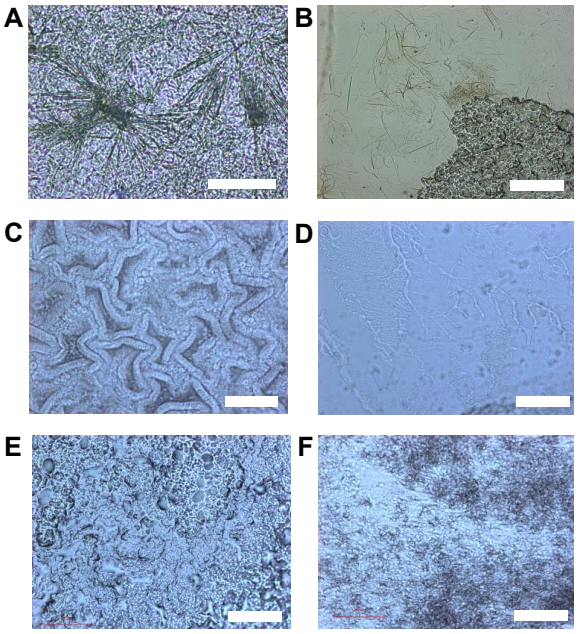

Figure S9. Optical microscopy images of DPPC (A, B), PBD-b-PEO (C, D), and 1:1 molar ratio of DPPC to PBD-b-PEO hybrid (E, F) films with 5 mol% PTX incorporated after 16 h of hydration. In case of lipid films (A, B), PTX crystals form bundles. Crystal formation was prominent in pure lipid films while polymer and hybrid films exhibited better capability of PTX incorporation. Scale bars: (A) 100 µm (B-F) 200 µm.